Atomic Structures of Benzene and Pyridine on Si(5 5 12)-2 × 1

Hojin Jeong,[†,‡] Sukmin Jeong,[‡] S. H. Jang,[‡,§] J. M. Seo,[†,‡] and J. R. Hahn*[,‡,§]

Departments of Physics and Chemistry and Institute of Photonics and Information Technology, Chonbuk National University, Jeonju 561-756, Korea

Received: April 3, 2006; In Final Form: June 22, 2006

The adsorption structures of benzene and pyridine on Si(5 5 12)-2 × 1 were studied at 80 K by using a low-temperature scanning tunneling microscope and density functional theory calculations. These structures are different from those observed on low-index Si surfaces: benzene molecules exclusively bind to two adatoms, that is, with di-σ bonds between carbon atoms and silicon adatoms, leading to the loss of benzene aromaticity; in contrast, pyridine molecules interact with adatom(s) through either Si−N dative bonding or di-σ bonds. Dative bonding configurations with pyridine aromaticity are the dominant adsorption features and are more stable than di-σ bonding configurations. Thus the dative bonding of nitrogen-containing heteroaromatic molecules provides a strategy for the controlled attachment of aromatic molecules to high-index surfaces.

I. Introduction

In recent years, research into the attachment of organic molecules to Si surfaces has been intensifying[1−3] because of potential applications of these systems in the construction of organic−silicon hybrid nanostructures that could be used in advanced microelectronics, biosensors, and optical devices. An understanding of the binding structures of the organic functional groups on these surfaces is crucial to such applications. For this reason, the chemisorption of organic molecules on Si has been the subject of many theoretical and experimental investigations.[3−39]

Aromatic molecules are of particular interest because they can be used as molecular nanowires or switches. Numerous studies have reported that unsaturated molecules react readily with the dangling bonds of clean silicon surfaces via cycloaddition reactions.[2−7] The prototypical aromatic molecules benzene and pyridine exhibit multiple bonding configurations on the Si(100) surface. In the case of benzene on Si(100),[8−18] all observed configurations are without aromaticity, which means the loss of functionality that is important in nanoelectronics. In addition to the configurations resulting from these cycloaddition reactions, molecules containing nitrogen have an additional available bonding configuration. The lone pair of electrons on the nitrogen atom can be donated to the silicon surface, resulting in stable chemisorbed species, as has been demonstrated for several saturated amines on Si(100) and Si(111), that is, in dative bonding.[19−21] This bonding geometry is of significant interest for aromatic heterocycles such as pyridine, because it preserves the aromaticity of the molecule. Previous experimental and theoretical studies of the adsorption of pyridine onto Si(100) have indicated that competitive adsorption between the dative and cycloaddition pathways is expected.[22,23] It was recently reported that pyridine on Si(100) initially binds via a dative bonding configuration and is then converted to a more stable bridging state without aromaticity.[24] Therefore, the ability to control the selectivity of adsorption on Si surfaces while preserving aromaticity is important for the design of molecule-based devices with tailored structures and electronic properties.

In the present study, we investigated and compared the adsorption structures of benzene and pyridine on a high-index Si surface, Si(5 5 12)-2 × 1. Few studies of the adsorption of organic molecules onto high-index Si surfaces have been reported[39] because of the relatively large size of their unit cells and their complicated reconstruction processes. The Si(5 5 12)-2 × 1 surface is interesting because of its peculiar and complex surface reconstructions. It is highly planar and one-dimensional (1-D) symmetric, and it contains single domains that do not cross each other. Because of the structural regularities of its 1-D chains and its hierarchy for metal adsorption, the Si(5 5 12)-2 × 1 surface has attracted significant attention as a template for fabricating 1-D metal nanowires with line widths on the true single-nanometer scale.[40−46] Although Si(100) is currently the dominant substrate for electronic device fabrication, the use of high-index Si surfaces as substrates in specialized applications is being investigated. Si(5 5 12)-2 × 1 is also of particular scientific interest because of its array of low-index terraces. The unique spatial arrangement of surface atoms and the redistribution of surface electrons provide a number of chemically, spatially, and electronically inequivalent reactive sites, including dimer, adatom, and tetramer sites and honeycomb chains. The comparison of the adsorption dynamics of each terrace is of significant scientific interest. We examined the adsorption structures of benzene and pyridine molecules on the Si(5 5 12)-2 × 1 surface using a low-temperature scanning tunneling microscope (STM) and density functional theory (DFT) calculations. We found that benzene binds strongly to two adatoms with di-σ bonds, destroying its aromaticity in the process. However, most pyridine molecules maintain their aromaticity when they interact with adatoms through Si−N dative bonding, which is more stable than di-σ bonding. $Si-N^1$ and $Si-C^4$ or $Si-C^2$ and $Si-C^5$ di-σ bonds can be formed.

II. Experimental and Theoretical Methods

The silicon samples used in this work, *n*-type Si(5 5 12) (P-doped), were ultrasonicated with ethyl alcohol. After overnight

* Corresponding authors: e-mail jsm@chonbuk.ac.kr (S.J.) or jrhahn@chonbuk.ac.kr (J.R.H.).
† Department of Physics.
‡ Institute of Photonics and Information Technology.
§ Department of Chemistry.

10.1021/jp062075g CCC: $33.50
Published on Web 07/27/2006

degassing at 700 °C in an ultrahigh vacuum (UHV) system with a pressure lower than 1×10^{-10} Torr, clean Si samples were prepared by using repeated cycles of 1 keV Ne^+ ion sputtering and flashing at 1500 K for 30 s. It was observed that during flashing at 1500 K excessive surface roughening occurred if the vacuum pressure exceeded 2×10^{-9} Torr. To maintain the pressure below 2×10^{-9} Torr during flashing, the sample heater was heavily degassed before flashing. After flashing, the sample was rapidly cooled to 1200 K and then cooled to room temperature at a rate of 2 K/s to promote surface reconstruction. The cleanliness of the samples was confirmed with a homemade STM.[39,47] The base pressure of the vacuum chamber was below 2×10^{-11} Torr. Benzene and pyridine (Aldrich Chemical) were further purified with several cycles of freeze−pump−thaw before being dosed onto the clean Si(5 5 12)-2 × 1 surface. Dosing was carried out through a leak valve equipped with a microcapillary-array filled tube to promote uniform adsorption onto the surface. The sample purity was checked with a mass spectrometer attached to the chamber. The surface coverages of the adsorbed molecules were kept below 0.01 monolayer (ML) by exposing the surface only when the chamber pressure was in the 10^{-11} Torr region. Electrochemically etched tungsten tips were prepared with repeated cycles of self-sputtering by using field emission in a Ne atmosphere and by e-beam heating in a strong electric field.

All calculations were performed with ultrasoft pseudopotentials[48] and the generalized-gradient approximation (GGA) for the exchange-correlation energy,[49] which are incorporated in the Vienna ab initio simulation package (VASP).[50] The surface was simulated with a repeated slab model consisting of four Si layers and a 10.0 Å vacuum layer. The bottom of the slab has a bulklike structure, with each Si atom saturated by H atom(s). The supercell has 4× periodicity along the chain direction, which limits interactions between the molecules adsorbed on the neighboring supercells; for this periodicity, the distance between adsorbed molecules is about 10 Å. We considered molecular adsorption on the D3 and D2 units (see below for explanation of this notation) of this large Si(5 5 12)-2 × 1 surface supercell with 4× periodicity. Since the spacings of the D1, D2, and D3 units are quite large (15.7, 22.1, and 15.7 Å, respectively), we treat them as independent surfaces, as discussed later in the paper. A cutoff energy of 20 Ry was used for the plane wave basis and the Γ point in the surface Brillouin zone (SBZ). Geometry optimization was carried out for all atoms until the remaining force acting on each ion was less than 0.005 eV/Å, except for the bottom-most H and Si atoms. The convergence tests showed that these computational parameters were sufficient to obtain converged results.[51] Increases in the number of *k*-points to four and in the cutoff energy to 30 Ry were also tested; the total differences between the energies of the two adsorption structures were found to be only 0.03 and 0.004 eV, relative to the 20 Ry Γ point value.

III. Results and Discussion

A. Atomic Structure of Si(5 5 12)-2 × 1. Figure 1 shows an ideal cross-section of the Si lattice viewed from the [1 $\bar{1}$ 0] direction. The distance from the origin (000) to the crossing point of each direction (*hhk*) is its periodic length along the direction perpendicular to the [1 $\bar{1}$ 0] direction. The inclined angles from (001) and corresponding perpendicular periodicities are listed in the inset table in Figure 1a. The (5 5 12) plane [shown as the solid line between (000) and (5 5 12)] is composed of the (7 7 17) and (337) planes. Furthermore, because the (7 7 17) plane consists of the (225) and (337) planes, the (5 5 12) plane can be decomposed into two (337) planes and one (225) plane. Similarly, the (225) plane can be decomposed into the (337) and (113) planes, and the (337) plane can be decomposed into the (112) and (113) planes. The angles of planes such as the (113), (225), (7 7 17), (337), and (112) planes with respect to the (5 5 12) plane are less than 5.3°, so their combinations have a high probability of being present in the reconstructed Si(5 5 12) surface. Baski et al.[43,45] proposed a model of reconstructed Si(5 5 12) consisting of a unit cell composed of two (337) planes and one (225) plane, and subsequent additional experimental results have confirmed the presence of this combination in the unit cell. However, due to the large unit cell size, 0.77 × 5.35 nm^2, and limited computing capacity, atomic structural models based upon various sets of experimental results have not been consistent. Of these models, one recent Si(5 5 12)-2 × 1 model was found to have the lowest energy, and so it was employed in the present study. When the bulk-terminated Si(5 5 12) surface reconstructs to reduce its surface free energy, the periodicity along the [$\bar{1}$ 10] direction becomes doubled with a unit of size 0.77 × 5.35 nm^2.

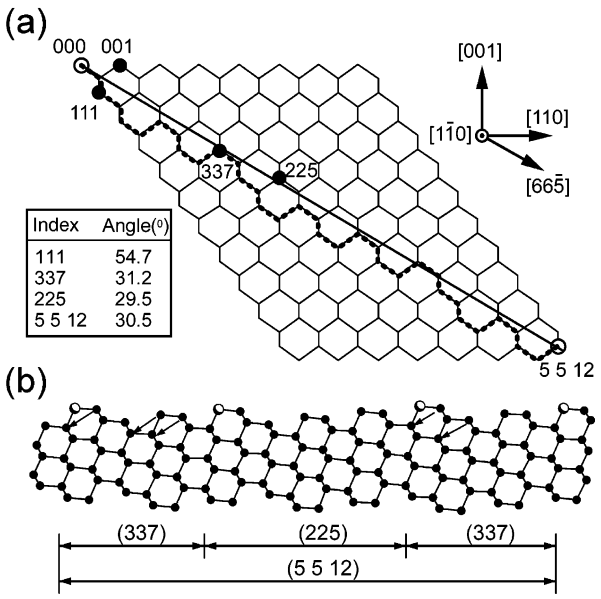

Figure 1. (a) Si lattice viewed from the [1 $\bar{1}$ 0] direction for several surface orientations with angles displayed in the inset table. The solid line between the two open circles indicates the (5 5 12) plane. The dotted line segments indicate the ideal bulk-terminated Si(5 5 12) surface. (b) The (5 5 12) surface is composed of three nearly parallel surfaces, (337), (225), and (337). The length of the (5 5 12) unit cell is 53.5 Å, and the lengths of the (337) and (225) units are 15.7 and 22.1 Å, respectively. The arrows in panel b indicate the bond-breaking and re-bonding required for construction of the structural model. The gray circles in panel b indicate the Si atoms that are removed for stable reconstruction.

Figure 2 shows a filled-state STM image of the Si(5 5 12)-2 × 1 surface and schematic drawings of the top and cross-sectional views. The model consists of three units [D1 (337), D2 (225), and D3 (337)] separated by honeycomb (H) chain boundary features. The D2 and D3 units contain a dimer facing buckled adatom row (D/A). A tetramer row structure (T) is present in the D1 and D2 units. The H chain separating the units has a 5−3−5 ring structure. D, A, and T have 2× periodicity. As a consequence of this reconstruction and the formation of the H chain, the number of dangling bonds is reduced to 22 from 48 in the bulk-terminated structure. Many defects were observed in the H chains separating D1 and D2. It was found that the three 1-D features (D1, D2, and D3) cyclically transform under local surface stresses (the tensile and

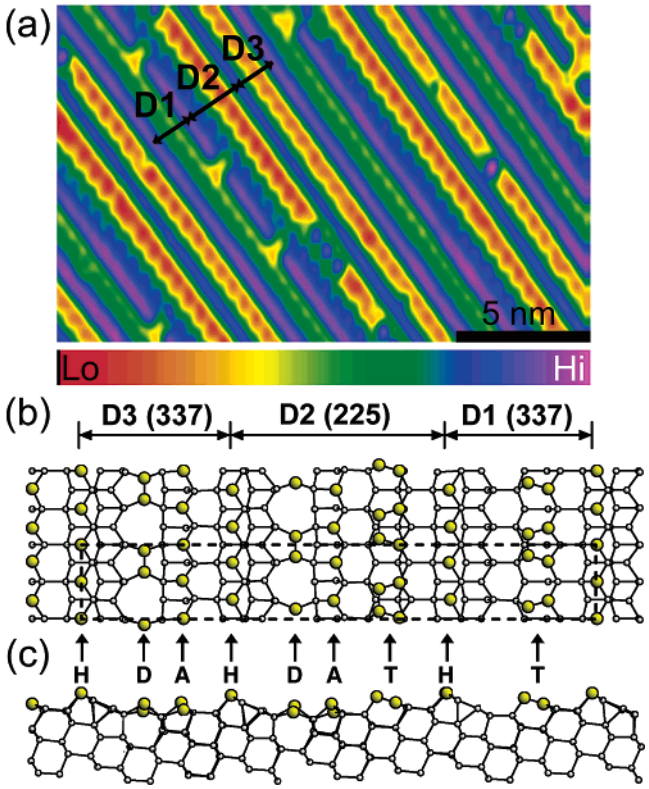

Figure 2. (a) Filled-state STM image of a Si(5 5 12)-2 × 1 surface. The image was obtained at a tunneling current of 0.5 nA, a sample bias voltage of −2.0 V, and a sample temperature of 80 K. The scan area is 20.0 × 12.5 nm^2. Full scale of the *z*-axis-bar is 2.2 Å. (b, c) Schematic drawings of top and cross-section views of the Si(5 5 12)-2 × 1 surface, respectively. One unit cell of Si(5 5 12)-2 × 1 consists of D1, D2, and D3 units, which are (337) with tetramer (T) and (225) and (337) with dimer facing adatom (D/A), respectively. The (225) unit contains D/A and T. The two (337) units and one (225) unit are separated by honeycomb (H) chain structures. Apart from the H chains, the rest of the one-dimensional structures have 2× periodicity. The rectangle (dashed lines) in panel b indicates the surface unit cell.

compressive stresses in the plane). Inhomogeneous environmental stress during reconstruction can lead to an imbalance between the tensile and compressive stresses, which results in the formation of line defects that reduce the surface energy.[42]

B. STM Investigation of Benzene and Pyridine on Si(5 5 12)-2 × 1. Benzene molecules were adsorbed onto the Si(5 5 12)-2 × 1 surface at a sample temperature of 80 K, and the resulting surface was investigated with STM. Figure 3a shows a representative topographical image (filled-state) obtained after benzene adsorption at a very low coverage (<0.01 ML). By comparison of this image with that of a clean surface, the (relatively) bright features in the image were attributed to adsorbed benzene molecules. The protrusions were classified into four different configurations according to their appearance, labeled a−d. These features increase in number as the exposure of benzene is increased, verifying that they are due to adsorbed molecules.

Features a and b on the D3 units appear as asymmetric protrusions along the [6 6 $\bar{5}$] direction. They appear slightly lower than the H chains in the topographical images (Figure 4) but are higher than D and A. Their asymmetric appearance is due to a tilted adsorbed benzene structure (see below). Features c and d are observed on the D2 units and are very similar to features a and b. The adsorption positions of a−d are determined as A (adatoms) of D3 or D2 units. Protrusions b and d (which are on the D3 and D2 units, respectively) are shifted along the

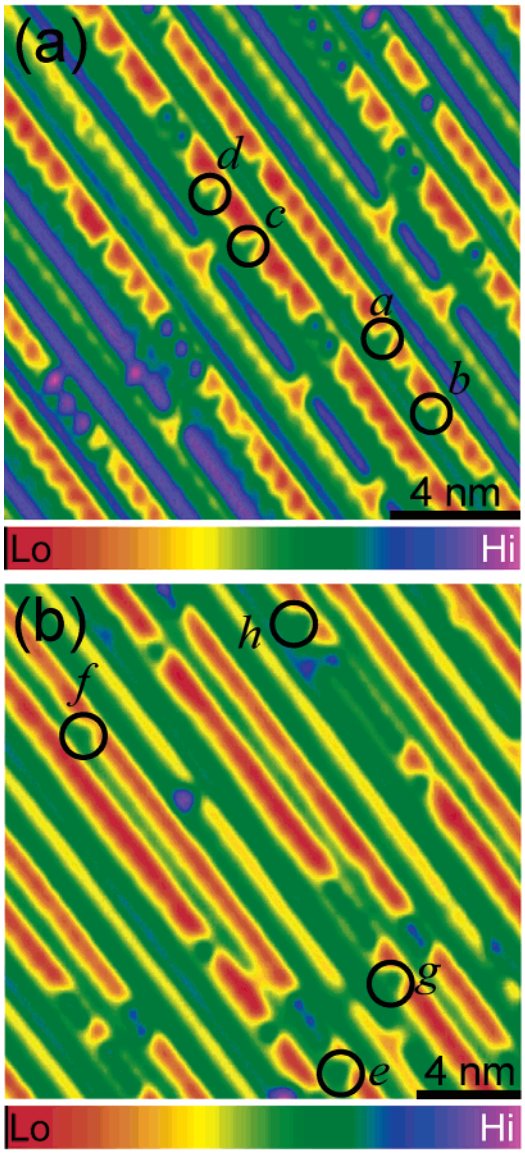

Figure 3. Filled-state STM images of Si(5 5 12)-2 × 1 surfaces with very low coverages of (a) benzene and (b) pyridine. The molecules were adsorbed at 80 K. Features a−d are due to benzene adsorption, and features e−h are due to pyridine. The images were obtained at a tunneling current of 0.5 nA, a sample bias voltage of −2.0 V, and a sample temperature of 80 K. The scan areas are 15.8 × 15.8 nm^2 (a) and 20.0 × 20.0 nm^2 (b). Full scales of the *z*-axis-bar are 2.3 Å (a) and 3.2 Å (b).

chain direction by 3.9 Å and are located near dimers. Other features (not shown) were observed on H chains separating D1 and D2 units with very low percentages. The fractional occurrences of the configurations at 80 K were counted by sampling 350 protrusions and are summarized in Table 1. This population distribution suggests that the benzene molecules adsorbed on the A site are in energetically more stable states than the configurations corresponding to other features.

In the case of pyridine molecules, four types of protruding features [e−h in Figure 3b] were observed. Features e and f are found on D3 units, and features g and h are found on D2 units. Their asymmetric appearance is due to a tilted adsorption structure (see below). The adsorption positions of e−h are determined to be adatoms of D3 and D2 units. The fractional occurrences of the e−h configurations at 80 K were counted by sampling 230 protrusions and are summarized in Table 1. This population distribution suggests that pyridine molecules

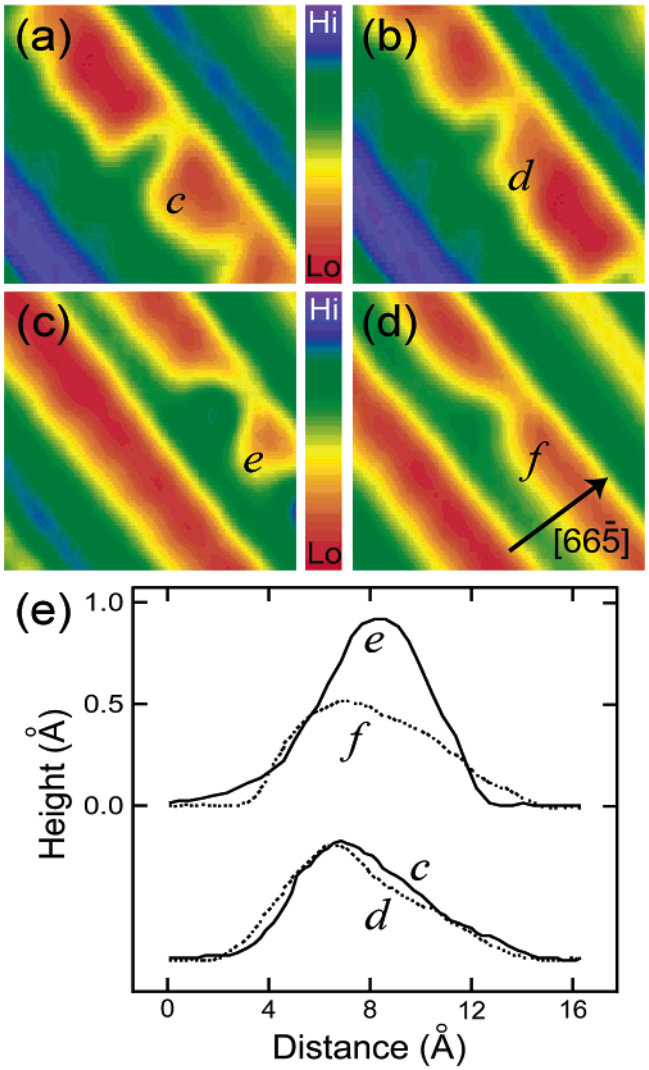

Figure 4. (a−d) Magnified STM images of features c−f in Figure 3; (e) corresponding cross-sectional cuts for each molecule along the [6 6 $\bar{5}$] direction. The background topography obtained from the clean surface was subtracted from the cross-sectional cuts.

TABLE 1: Relative Populations of Various Benzene and Pyridine Configurations Counted from STM Images[a]

configuration	rel population (%)
a	21
b	17
c	31
d	27
others[b]	5
e	45
f	3
g	40
h	3
others	4

[a] See Figure 3 for the labeling scheme. [b] Reference 39.

adsorbed on the A site corresponding to features e and g are in energetically much more stable states than other configurations.

Figure 4 shows magnified images of the most dominant features, c−f, and their cross-sectional cuts along the [6 6 $\bar{5}$] direction. To remove the effect of the surface topography on the molecular images, a background topography was obtained for clean areas of the surface and subtracted from the cuts. In the topographic image, benzene and pyridine appear as slightly elongated protrusions with slightly different heights along the [6 6 $\bar{5}$] direction of the surface. The maximum heights of the benzene features c and d are ∼0.5 Å. No measurable differences were observed between c and d. However, the height of pyridine feature e (∼1 Å) is higher than that of feature f. The maximum height of feature f is comparable to those of the benzene features. The maximum heights of a, b, g, and h (Figure 3) are similar to those of c, d, e, and f, respectively.

TABLE 2: Adsorption Energies of Various Configurations of Benzene and Pyridine on Si(5 5 12)-2 × 1 and the Corresponding Features in the STM Images[a]

configuration	E_{ad} (eV)	STM
benzene		
D3-A_1(b)	1.20	a
D3-A_2(b)	1.11	b
D3-D_1(b)	0.86	
D3-D_2(b)	0.29	
D3-H_1(b)	0.22	
D2-A_1(b)	1.14	c
D2-A_2(b)	1.03	d
D2-D_1(b)	0.82	
D2-T_1(b)	0.46	
pyridine		
D3-A_1(p)	1.64	e
D3-A_2(p)	1.62	
D3-A_3(p)	1.35	f
D3-A_4(p)	1.21	f*
D3-D_1(p)	1.05	
D3-D_2(p)	0.95	
D3-H_1(p)	0.67	
D3-H_2(p)	0.47	
D3-DA_2(p)	1.19	
D1-T_1(p)	1.25	
D1-T_2(p)	0.73	

[a] STM images are shown in Figure 3. See text for explanation of notation.

C. DFT Calculations of the Adsorption Structures of Benzene and Pyridine on Si(5 5 12)-2 × 1. To understand the STM images presented in the previous section, we performed DFT calculations to search for the stable adsorption configurations of benzene and pyridine molecules on the Si(5 5 12)-2 × 1 surface. We considered all possible structures of molecular adsorption and calculated their adsorption energies through the geometry optimization of these structures. The adsorption energies of some representative structures for benzene and pyridine are listed in Table 2 and were calculated as $E_{ad} = E_{clean} + E_{mole} - E_{struc}$, where E_{clean}, E_{mole}, and E_{struc} are the total energies of the clean surface, the benzene and pyridine molecules, and the adsorbed structure, respectively.

The most stable adsorption structure for benzene was found to be D3-A_1(b) with E_{ad} = 1.20 eV, in which the benzene molecule binds with two adatoms between the dimers (Figure 5a). This structure is characterized by the formation of two σ-bonds with the substrate and two C═C double bonds in the benzene molecule. The formation of the double bonds was confirmed by comparing the bond lengths: the bond length of 1.35 Å for C═C is smaller than the lengths of 1.50 Å for the C−C single bond of the adsorbed benzene molecule and 1.40 Å for C═C in free benzene molecules. The distance between C^1 and C^4 is 2.95 Å, which is greater than that of the free molecule (2.78 Å) due to the larger Si−Si distance (3.86 Å) of the substrate.

The second stable adsorption structure on the D3 unit is D3-A_2(b) (Figure 5b), in which the benzene molecule is shifted along the chain direction by ∼3.86 Å and is located near a Si dimer. The adsorption energy of D3-A_2(b) is smaller than that of D3-A_1(b) by 0.09 eV. This is due to the effect of stress on the substrate-adsorbed molecule system. Since the diagonal distance

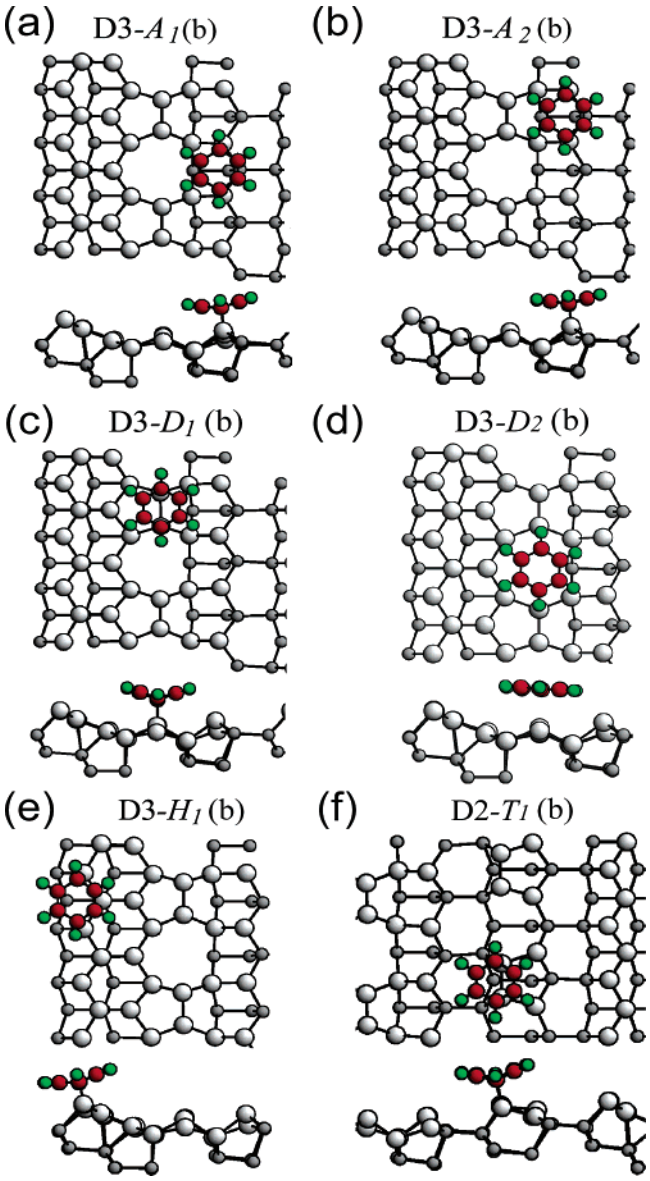

Figure 5. Equilibrium atomic structures of benzene molecules adsorbed on the D3 and D2 units of Si(5 5 12)-2 × 1. (a, b) Benzene adsorbed on two adatoms between two dimers of a D3 unit [D3-A_1(b) and D3-A_2(b)]. The configuration of benzene molecules is like a tilted butterfly. (c−f) Benzene adsorbed on dimers [D3-D_1(b) and D3-D_2(b)], honeycomb [D3-H_1(b)], and tetramer structures [D2-T_1(b)]. The gray circles represent silicon atoms; the red (green) circles represent carbon (hydrogen) atoms.

of the free benzene molecule (2.78 Å) is much smaller than the lattice constant along the chain direction (3.86 Å, as calculated with a cutoff of 20 Ry and GGA), the adsorbed molecule exerts compressive stress on the substrate. The nearby Si dimer also produces a compressive stress along the same direction, resulting in alignment of the compressive stress perpendicular to the dimer axis. This is in contrast to the D3-A_1(b) configuration, for which the compressive stress is arranged in a zigzag pattern to relieve stress. Indeed, this is observed in the Si(100) surface, for which the $p(2 \times 2)$ reconstruction has a lower energy than the buckled $p(2 \times 1)$ reconstruction. The structural parameters of the adsorbed benzene molecule in D3-A_2(b) are effectively the same as those in D3-A_1(b), within 0.01 Å.

The structure consisting of a benzene molecule on the dimer line D3-D_1(b) Figure 5c) has a smaller adsorption energy than the D3-A_1(b) structure by 0.34 eV. When the benzene molecule adsorbs on the dimer in a different way, for example, the binding of C^1 and C^2 with the substrate, the resulting structure has lower stability than the D3-D_1(b) structure. It is not possible for benzene to adsorb on neighboring dimers such as D3-D_2(b), due to the resulting large stress in the benzene molecule. Other structures such as D3-H_1(b) (Figure 5e) also have low adsorption energies. These low adsorption energies can be understood in terms of the local geometry of the substrate near the adsorbed benzene molecule. For example, the bond angles of the Si atom bonded with the C atom range from 97° to 120°, that is, far from the angle (109.5°) of sp^3 hybridization, which results in a high strain energy. In contrast, the corresponding bond angles in the stable D3-A_1(b) structure are between 108° and 111°.

Adsorption of benzene on D2 units is very similar to adsorption on D3 units. The adsorption energies only differ by 0.06 eV and the energy ordering is unchanged. Thus adsorption need only be discussed for one of these two units to characterize the adsorption behaviors of benzene on the whole Si(5 5 12)-2 × 1 surface. However, additional calculations are needed for the D2 unit since it contains the tetramer, which does not appear in the D3 unit. The most stable adsorption configuration on the tetramer is D2-T_1(b), which has an adsorption energy of 0.46 eV (Figure 5f). This structure is also characterized by the formation of two σ-bonds with the substrate and two C═C double bonds in the benzene molecule.

The adsorption structures of pyridine on the Si(5 5 12)-2 × 1 surface are different than those of benzene. Figure 6 shows the stable structures we investigated. The most stable structure on D3 units is D3-A_1(p), which has an adsorption energy of 1.64 eV (Table 2). In this structure, the pyridine molecule binds with the surface vertically through nitrogen and adatom bonding with a tilted geometry (vertical configuration). The total energy changes by less than ∼0.04 eV as the molecular ring rotates around the N−adatom bond, which implies that the pyridine molecule can rotate nearly freely. The next most stable adsorption structure on D3 units is D3-A_2(p) (not shown), in which the pyridine is shifted along the chain direction by ∼3.86 Å and is located near a Si dimer. The adsorption energy of D3-A_2(p) (1.62 eV) is very similar to that of D3-A_1(p).

Other possible adsorption structures are parallel configurations, similar to the tilted butterfly configuration of benzene, in which two σ-bonds with the substrate are formed, 1,4-di-σ [D3-A_3(p)] and 2,5-di-σ [D3-A_4(p)]. Our total energy calculations show that the vertical configuration is more stable than the parallel configurations. The same trend is found for other adsorption sites such as the dimer, honeycomb chain, and tetramer sites, as shown in Table 2. This result is in agreement with those of cluster calculations for pyridine adsorption on Si(100)-2 × 1.[52] This is very interesting because the parallel configuration has fewer dangling bonds than the vertical configuration. The adsorption energy decreases along the sequence of adatom, dimer, and honeycomb chain, which results from structural effects (see below). On the dimer, tetramer, and honeycomb sites (not shown) only the parallel configurations are found (Figure 6d−f), as is the case for benzene. It is interesting that the parallel configuration with bonding between an adatom and a dimer has a higher adsorption energy, 1.19 eV [D3-DA_1(p)].

D. Binding Structures of Benzene and Pyridine on Si(5 5 12)-2 × 1. The adsorption positions of the molecules can be determined by comparing the STM images (Figures 3 and 4) with schematic diagrams of the Si(5 5 12)-2 × 1 structure (Figure 2). On the basis of the STM analysis and our theoretical investigations, we assigned species a and b in Figure 3a to D3-A_1(b) and D3-A_2(b), respectively. Protrusions c and d are due

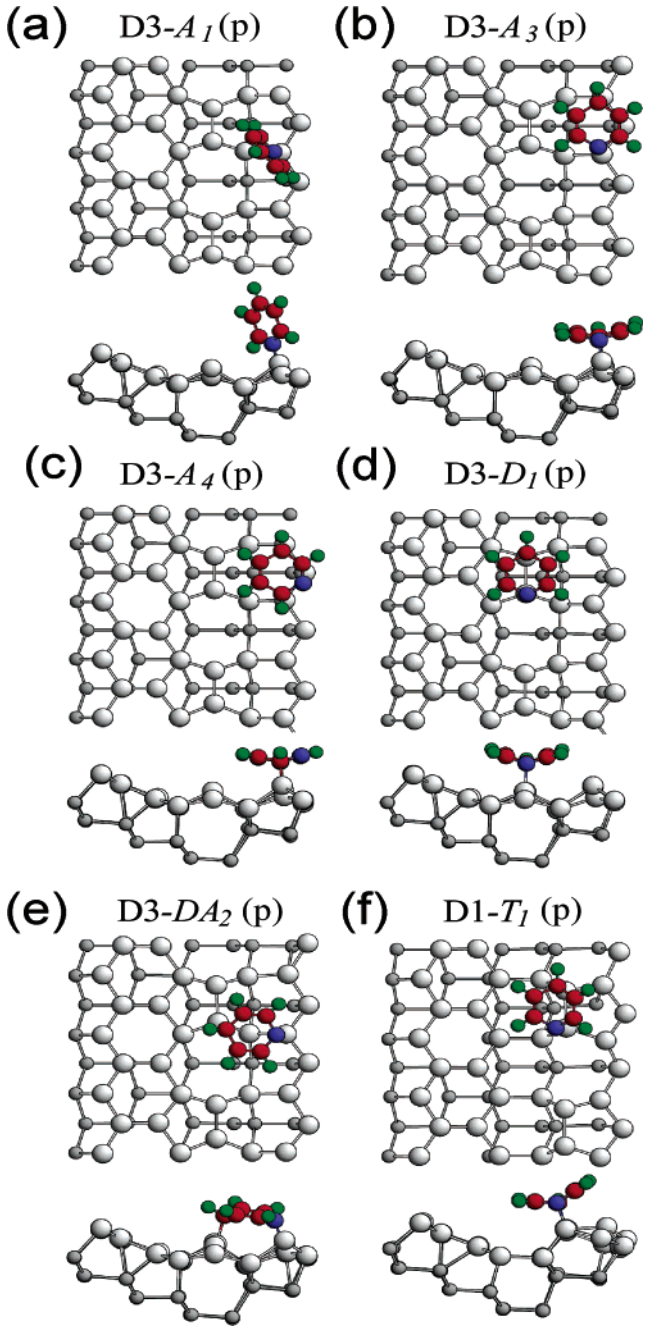

Figure 6. Equilibrium atomic structures of pyridine molecules adsorbed on the D3 and D1 units of Si(5 5 12)-2 × 1. (a) Pyridine vertically adsorbed on an adatom of D3 [D3-A_1(p)]. (b, c) Pyridine adsorbed in a parallel configuration on two adatoms between two dimers of a D3 unit [D3-A_3(p) and D3-A_4(p)]. (d) Pyridine adsorbed in a parallel configuration on a dimer of a D3 unit [D3-D_1(p)]. (e) Pyridine adsorbed in a parallel configuration between a dimer and adatom of a D3 unit [D3-DA_2(p)]. (f) Pyridine adsorbed in a parallel configuration on a tetramer of a D1 unit [D3-T_1(p)]. Gray (blue) circles represent silicon (nitrogen) atoms; red (green) circles represent carbon (hydrogen) atoms.

to D2-A_1(b) and D2-A_2(b), respectively. The calculated energetics of the various benzene configurations are qualitatively consistent with our experimental findings: the population of benzene molecules adsorbed on adatom states (96%) is much higher than those of other configurations (4%).[39] The very low populations of other configurations may be due to their very low adsorption energies. Adsorption on D and T sites was not observed with the STM imaging. It is possible that adsorption occurs on the dimer or tetramer atoms but that the benzene molecules then diffuse to the A site.

For pyridine molecules, species e and f in Figure 3b were attributed to D3-A_1(p) and D3-A_3(p) [or D3-A_4(p)] on the D3 unit, respectively. The position of the nitrogen atom in the tilted butterfly structure cannot be resolved with the STM image. Therefore species f is either D3-A_3(p) or D3-A_4(p). Similarly, species g and h in Figure 3b were attributed to D2-A_1(p) and D2-A_3(p) [or D2-A_4(p)] on the D2 unit (not shown in Figure 6). The higher population (85%) of the vertical configurations (e and g) than of other configurations is due to their higher adsorption energies (Table 2). In addition, the larger maximum height of feature e (Figure 4e) than that of f is consistent with this assignment, since the vertical configuration should lead to a higher protrusion in the STM image. Assuming that equilibrium was reached at the present experimental temperature (80 K), the energy difference between A and H sites for benzene adsorption was calculated to be only 0.02 eV. This low energy difference suggests that the migration of molecules upon adsorption between adsorption sites may play a role in determining the adsorption site.

It is interesting that the vertical configuration of pyridine bonding with an adatom is more stable than the parallel configurations. In the free pyridine molecule with its 6π aromatic ring, the calculated N^1-C^2, C^2-C^3, and C^3-C^4 bond lengths are 1.35, 1.40, and 1.39 Å, respectively. In the vertical configurations, these bond lengths are only slightly different (±0.01 Å) and the ring has a planar structure, indicating that the aromaticity of the ring is maintained. In the parallel configurations, on the other hand, two double bonds between C^2 and C^3 (1.34 Å) and C^5 and C^6 (1.34 Å) are formed, which leads to the loss of aromaticity. This difference explains the higher stability of the vertical configuration. In addition, the greater stability of the adatom sites is due to the strain around the Si atom bound to nitrogen. In the vertical configuration, indeed, the bond angles are within 108.5° ± 1.7°, close to the angle 109.5° of the sp^3 bond configuration, but in the other configurations the corresponding bond angles are far from the sp^3 bond configuration.

We calculated the spatially resolved local density of states (LDOS) of molecules on the surface for all configurations in order to facilitate the interpretation of the STM images. These are electron isodensity contours that are obtained by integrating the LDOS between the bias voltage and Fermi level (the Tersoff−Hamann method).[53] The results correspond to a constant-current image with an ideal tip located at a certain height above the surface. The calculations did not take into account the LDOS of the tip, the tunneling probability, or the tip−surface interactions. Therefore, they are expected to be different from the experimental STM image. Figure 7 shows the calculated LDOS maps (filled-state) for D3-A_1(b), D2-A_1(b), D3-A_1(p), and D3-A_3(p) and the corresponding structural models. The filled-state mapping shows that the parallel configurations for adsorbed benzene and pyridine molecules appear as protrusions with an asymmetric dumbbell shape. The vertical configuration appears as an asymmetric protrusion. The π states of the C=C bonds of benzene and pyridine produce these protruding features. Since the parallel configurations are tilted, the protrusions on the honeycomb (tetramer) side of the D3-A_1(b) and D3-A_3(p) [D2-A_1(b)] configurations are slightly higher. The experimental STM filled-state image contains asymmetric protrusions. With the consideration that insufficient STM resolution was obtained because the tip apex is larger than the molecule, the STM images of adsorbed benzene and pyridine are qualitatively consistent with the theoretical predictions. It should also be mentioned that the apparent heights of atoms

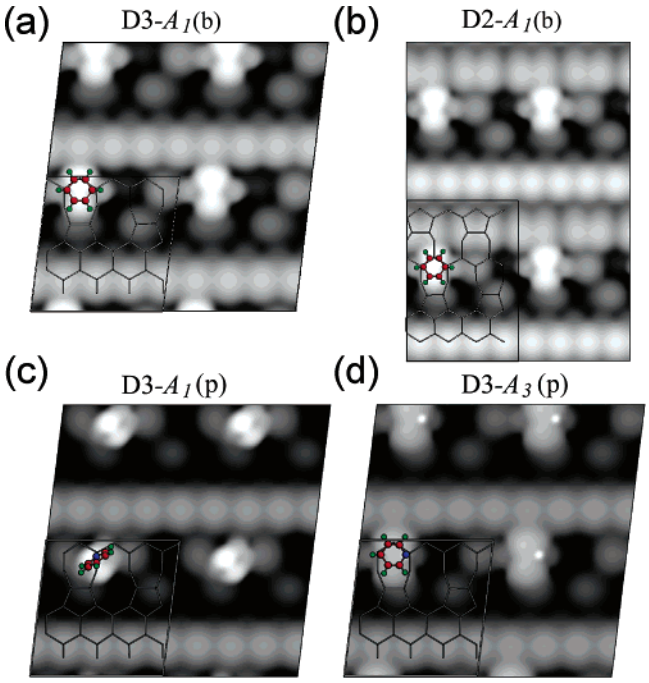

Figure 7. Spatially resolved local density of electronic states (filled state at −2.0 V) for stable benzene [(a) D3-A_1(b) and (b) D2-A_1(b)] and pyridine structures [(c) D3-A_1(p) and (d) D3-A_3(p)]. The black lines shown inside the image indicate the corresponding structural models. Gray (blue) circles represent silicon (nitrogen) atoms; red (green) circles represent carbon (hydrogen) atoms.

and molecules in the STM image are likely to be different from the calculated results, since our calculations did not take the tip states into account.

E. Comparison with Adsorption Structures on Low-Index Si Surfaces. Many experimental and theoretical investigations have shown that unsaturated organic compounds such as ethylene and 1,3-cyclohexadiene can react with the Si(100) surface via mechanisms that are analogous to the [2 + 2] and [4 + 2] cycloaddition reactions of organic chemistry.[2−7] Some aromatic molecules such as benzene,[8−18] xylene,[25] and toluene[25,26] undergo adsorption accompanied by a loss of aromaticity. However, some functionalized aromatic molecules such as styrene[27] and phenyl isothiocyanate[28] interact with Si(100) with a high degree of selectivity. Furthermore, molecules containing nitrogen atoms are of particular interest because their lone-pair electrons are good electron donors, giving these compounds particularly useful chemical and electrical properties. It was recently observed that pyridine on Si(100) initially binds via a dative bonding configuration but is converted to a more stable bridging state without aromaticity.[24]

The binding structures of benzene and pyridine on Si(5 5 12)-2 × 1 differ from those observed on low-index surfaces such as Si(100)[8−18] and Si(111).[29−35] Benzene adsorbs on an adatom-rest atom pair of Si(111)-7 × 7 and on dimer structures of Si(100)-2 × 1 through a precursor state. On the Si(111)-7 × 7 surface, benzene molecules adsorb as a 1,4-cyclohexadiene chemisorbed benzene forming two σ-bonds to adjacent adatom and rest atom Si sites through [4 + 2]-like or [2 + 2]-like cycloadditions, with a binding energy of 0.95 eV. On Si(100)-2 × 1, benzene adsorbs on top of the Si(100) surface dimer rows to avoid energetically disfavored structures. Among the structures proposed in the literature as the lowest-energy configuration is the tetra-σ-bonded structure characterized by one C═C double bond and four C−Si bonds.[8−10] The 1,4-cyclohexadiene-like configuration, in which the benzene molecule is di-σ-bonded to the two dangling bonds of the same Si surface dimer, was proposed as a metastable adsorption state. In the present study, however, no metastable states were observed at 80 K. The observed adsorption states were found to be stable even during scanning at a higher bias voltage (∼3.0 V bias voltage at 1 nA tunneling current), which implies that there is a stronger binding of benzene and pyridine on adatoms of Si(5 5 12)-2 × 1 than on dimers of Si(100)-2 × 1. In addition, a control experiment at room temperature produced similar structures. The adsorption mechanism of benzene with adatoms of Si(5 5 12)-2 × 1 may be different from that of the formation of cycloadduct on Si(100) because no π bonds exist between adatoms and the separation of adatoms (3.86 Å) is larger than that of the Si dimer atoms of Si(100) (2.3 Å).

Si(100) dimers act as electron acceptors, as expected for the interaction of nitrogen-containing molecules such as ammonia,[36,37] pyridine,[37] and $C_6H_5NH_2$[38] with Si surfaces. Theoretical calculations suggest that the interaction between the lone pair of electrons on a N atom and one atom of a Si dimer via a transient dative bond weakens the N−H bond and thus induces dissociative adsorption. A similar mechanism has been proposed for other NH-containing molecules. These results showed that the formation of a dative bond with NH-containing molecules is competitive but that dissociative adsorption via the cleavage of the N−H bond is thermodynamically more favorable.

IV. Conclusions

We examined the stable adsorption structures of benzene and pyridine molecules on Si(5 5 12)-2 × 1 using STM imaging and DFT calculations. Several distinct adsorption structures were found. The benzene molecule adsorbs most strongly on two adatoms on the D3 and D2 units in a tilted butterfly configuration, which consists of di-σ bonds between C atoms and Si adatoms and two C═C double bonds in the benzene molecule. Pyridine molecules interact with adatom(s) on the D2 and D3 units through both Si−N dative bonding and di-σ bonds (either 1,4 di-σ or 2,5 di-σ). The former structure preserves aromaticity and is the dominant species because of its higher adsorption energy. Dative bonding between unsaturated organic molecules and high-index Si surface atoms could be useful for establishing a new strategy for the fabrication of organic molecular devices. Our results show that the Si(5 5 12)-2 × 1 surface can be used as a template for 1-D nanowires of nitrogen-containing molecules via dative interactions.

Acknowledgment. This paper is based upon work supported by Korea Research Foundation Grant (KRF-2004-005-C00001 and KRF-2003-070-C00026). This work was done while J.R.H. was visiting KIAS in Seoul during the winter of 2005 and 2006; gratitude is expressed to the institute. All calculations were performed by use of supercomputers at the Korea Institute of Science and Technology Information (KISTI).

References and Notes

(1) Waltenburg, H. N.; Yates, J. T., Jr. *Chem. Rev.* **1995**, *95*, 1589.
(2) Wolkow, R. A. *Annu. Rev. Phys. Chem.* **1999**, *50*, 413.
(3) Hamers, R. J.; et al. *Acc. Chem. Res.* **2000**, *33*, 617.
(4) Bent, S. F. *Surf. Sci.* **2002**, *500*, 879.
(5) Buriak, J. M. *Chem. Rev.* **2002**, *102*, 1271.
(6) Bozack, M. J.; Taylor, P. A.; Choyke, W. J.; Yates, J. T. *Surf. Sci.* **1986**, *177*, 933.
(7) Yoshinobu, J.; Tsuda, H.; Onchi, M.; Nishijima, M. *J. Chem. Phys.* **1987**, *87*, 7332.
(8) Hofer, W.; Fisher, A. J.; Lopinski, G. P.; Wolkow, R. A. *Phys. Rev. B* **2001**, *63*, 085314.
(9) Silvestrelli, P. L.; Ancilotto, F.; Toigo, F. *Phys. Rev. B* **2000**, *62*, 1956.

(10) Alavi, S.; et al. *Phys. Rev. Lett.* **2000**, *85*, 5372.
(11) Borovsky, B.; Krueger, M.; Ganz, E. *Phys. Rev. B* **1998**, *57*, R4269.
(12) Gokhale, S.; et al. *J. Chem. Phys*. **1998**, *108*, 5554.
(13) Lopinski, G. P.; Moffatt, D. J.; Wolkow, R. A. *Chem. Phys. Lett*. **1998**, *282*, 305.
(14) Taguchi, Y.; et al. *J. Chem. Phys.* **1991**, *95*, 6870.
(15) Liu, Q.; Hoffmann, R. *J. Am. Chem. Soc.* **1995**, *117*, 4082.
(16) Zhou, R. H.; Cao, P. L.; Lee, L. Q. *Phys. Rev. B* **1993**, *47*, 10601.
(17) Widdra, W.; Huang, C.; Yi, S. I.; Weinberg, W. H. *J. Chem. Phys.* **1996**, *105*, 605.
(18) Taylor, P. A.; et al. *J. Am. Chem. Soc.* **1992**, *114*, 6754.
(19) Cao, X.; Hamers, R. J. *J. Am. Chem. Soc.* **2001**, *123*, 10988.
(20) Mui, C.; Han, J. H.; Wang, G. T.; Musgrave, C. B.; Bent, S. F. *J. Am. Chem. Soc*. **2002**, *124*, 4027.
(21) Cao, X.; Hamers, R. J. *Surf. Sci.* **2003**, *523*, 241.
(22) Tao, F.; Ming, H. Q.; Wang, Z. H.; Xu, G. Q. *J. Phys. Chem. B* **2003**, *107*, 6384.
(23) Kim, H.-J.; Cho, J.-H. *J. Chem. Phys.* **2004**, *120*, 8222.
(24) Miwa, J. A.; Eves, B. J.; Rosei, F.; Lopinski, G. P. *J. Phys. Chem. B* **2005**, *109*, 20055.
(25) Coulter, S. K.; Hovis, J. S.; Ellison, M. D.; Hamers, R. J. *J. Vac. Sci. Technol. A* **2000**, *18*, 1965.
(26) Borovsky, B.; Krueger, M.; Ganz, E. *J. Vac. Sci. Technol. B* **1999**, *17*, 7.
(27) Schwartz, M. P.; Ellison, M. D.; Coulter, S. K.; Hovis, J. S.; Hamers, R. J. *J. Am. Chem. Soc.* **2000**, *122*, 8529.
(28) Ellison, M. D.; Hamers, R. J. *J. Phys. Chem. B* **1999**, *103*, 6243.
(29) Macpherson, C. D.; Leung, K. T. *Phys. Rev. B* **1995**, *51*, 17995.
(30) Li, Z.-H.; Li, Y.-C.; Wang, W.-N.; Cao, Y.; Fan, K.-N. *J. Phys. Chem. B* **2004**, *108*, 14049.
(31) Carbone, M.; et al. *Phys. Rev. B* **2000**, *61*, 8531.
(32) Brown, D. E.; Moffatt, D. J.; Wolkow, R. A. *Science* **1998**, *279*, 542.
(33) Cao, Y.; et al. *J. Phys. Chem. B* **1999**, *103*, 5698.
(34) Petsalakis, I. D.; Polanyi, J. C.; Theodorakopoulos, G. T. *Surf. Sci*. **2003**, *544*, 162.
(35) Lu, X.; Wang, X.; Yuan, Q.; Zhang, Q. *J. Am. Chem. Soc*. **2003**, *125*, 7923.
(36) Fattal, E.; Radeke, M. R.; Reynolds, G.; Carter, E. A. *J. Phys. Chem. B* **1997**, *101*, 8658.
(37) Wisjaja, Y.; Mysinger, M. M.; Musgrave, C. B. *J. Phys. Chem. B* **2000**, *104*, 2527.
(38) Cao, S.; et al. *J. Phys. Chem. B* **2001**, *105*, 3759.
(39) Hahn, J. R.; Jeong, H.; Jeong, S. *J. Chem. Phys.* **2005**, *123*, 244702.
(40) Jeong, S.; Jeong, H.; Cho, S.; Seo, J. M. *Surf. Sci.* **2004**, *557*, 183.
(41) Cho, S.; Seo, J. M. *Surf. Sci.* **2004**, *565*, 14.
(42) Kim, H.; Cho, Y.; Seo, J. M. *Surf. Sci.* **2005**, *583*, 265.
(43) Baski, A. A.; Erwin, S. C.; Whitman, L. J. *Science* **1995**, *269*, 1556.
(44) Peng, Y.; Minoda, H.; Tanishiro, Y.; Yagi, K. *Surf. Sci*. **2001**, *493*, 508.
(45) Baski, A. A.; Erwin, S. C.; Whitman, L. J. *Surf. Sci.* **1997**, *392*, 69.
(46) Peng, Y.; et al. *Surf. Sci.* **2001**, *493*, 499.
(47) Hahn, J. R. *Bull. Korean Chem. Soc.* **2005**, *26*, 1071.
(48) Vanderbilt, D. *Phys. Rev. B* **1990**, *41*, R7892.
(49) Perdew, J. P. *Electronic Structure of Solids '91*; Ziesche, P., Eschrig, H., Eds.; Academie Verlag: Berlin, 1991.
(50) (a) Kresse, G.; Hafner, J. *Phys. Rev. B* **1993**, *47*, R558. (b) Kresse, G.; Furthmuller, *Phys. Rev. B* **1996**, *54*, 11169.
(51) Kim, K. Y.; Song, B. K.; Jeong, S.; Kang, H. *J. Phys. Chem. B* **2003**, *107*, 11987.
(52) Li, Q.; Leung, K. T. *Surf. Sci.* **2003**, *541*, 2003.
(53) Tersoff, J.; Hamann, D. R. *Phys. Rev. Lett.* **1983**, *50*, 1998.